CONF-850706--5

LA-UR-85-769

LA-UR--85-769

DE85 009593

TITLE. MODELING HETEROGENEOUS HIGH EXPLOSIVE BURN WITH AN
EXPLICIT HOT-SPOT PROCESS

AUTHOR(S) Pier K. Ting
James N. Johnson
Charles A. Forest

SUBMITTED TO. The 8th Symposium (International) on Detonation, July 15-19, 1985
Albuquerque, N.M.

DISTRIBUTION OF THIS DOCUMENT IS UNLIMITED

Los Alamos
Los Alamos National Laboratory
Los Alamos, New Mexico 87545

FORM NO 836 R4

MODELING HETEROGENEOUS HIGH EXPLOSIVE
BURN WITH AN EXPLICIT HOT-SPOT PROCESS

P. K. Tang, J. N. Johnson, and C. A. Forest
Los Alamos National Laboratory
Los Alamos, New Mexico

We present a method of treating high explosive burn with a multi-step
process which includes the hot-spot excitation, decomposition, and the
propagation of reaction into the region outside the hot spots. The basic
features of this model are the separation of the thermal-mechanical and chemical
processes, and the partition of the explosive into hot spots and the region
exclusive of the hot spots. The thermal-mechanical aspects are formulated in a
way similar to the chemical process. The combined processes lead to a set of
rate equations for the mass fractions of reactants, intermediate states, and
final products. The rates are expressed initially in terms of general
characteristic times, but with specific phenomenological correlations introduced
in the final model. Computational examples are given of simulated flyer plate
impacts, short-shock initiation, corner turning, and shock desensitization.

INTRODUCTION

The rapid burning of high explosives (HE)
involves many complex thermal-mechanical and
chemical processes. Here the term burn refers
to the chemical energy release process
associated with shock initiation; also, the
thermal-mechanical process includes both
hydrodynamics and transport. In the classical
model of steady detonation, transport
processes are not considered in detail since
the shock thickness is quite small compared to
any typical dimension; second, the chemical
reaction rate is quite high and thus the
reaction zone is thin, and the entire process
is hydrodynamically controlled. Use of the
Rankine-Hugoniot relations and the Chapman-
Jouguet condition leads to a well-defined
detonation velocity(1). This model ignores
the chemical and transport aspects and thus
simplifies the problem significantly. A large
class of explosives follows this
simplification with a constant detonation
velocity under various conditions, provided
the size of the explosive region is much
greater than some characteristic dimension.
The classical burn model, based on ideal
steady detonation and known as programmed
burn, has been used successfully in many
engineering design applications.

With the advent of insensitive high
explosives (IHE), the chemical reaction can no

longer be assumed very fast compared to the
hydrodyramic process, especially for
initiation; in fact, the chemical process
could be so sensitive to local instantaneous
conditions that it may not start or reach
completion within the time of interest, at
least for a large portion of the HE. The
above condition is called detonation failure.
For the scenerios of shock-to-detonation
transition, HE encountering a weak shock will
undergo chemical reaction at some distance
behind the shock front, the effect of reaction
will propagate through the additional distance
to reach the front, intensifying and speeding
it up until a final steady detonation is
established. The total distance traversed by
the shock to the point of detonation is known
as the run. Obviously a weak initial shock
requires a long run. The finite distance
needed for the transition is nothing but an
indication of the finite reaction rate
involved. The unique experimental
relationship between the initial shock
pressure and the run distance is presented in
the form of a Pop plot. This relationship is
usually linear on a log-log scale(2) and is
used in the determination of the Forest-Fire
reaction rate(3).

While many recognize that models of HE
burn should be based on first principles,
there are numerous difficulties with this
approach. Even though the chemical

composition of the HE is usually known for the major constituents, the chemical processes that lead to the final products are poorly understood, and many intermediate species and some final products have not yet been identified. All of these make the description of the processes according to the principles of chemical kinetics almost impossible. The second difficulty in describing HE burn is that most solid HE's are not homogeneous; voids and cracks are present and distinct boundaries exist between various constituents. Physical heterogeneity requires mass and energy balance calculations among all components and phases if we are to describe the complete scenarios following the principles of continuum mechanics and chemical thermodynamics. The condition of extreme pressure during the burn adds more uncertainty in the determination of transport and thermal properties. In coupling with the detailed chemistry, the task of establishing a complete thermal-mechanical and chemical model appears impractical if not impossible. The motivation for the development of a new model is to avoid detailed calculations, but to include some essential physical concepts that a first-principles approach would contain. We consider this a compromise, but believe it offers many advantages and features frequently needed in computational models. The separation of thermal-mechanical and chemical processes, plus the partition of the HE into hot spots and the region other than hot spots are the main features of this model. The special attention paid to the treatment in the hot-spot region lends the name to the model, explicit hot-spot process. Details of the model have been presented elsewhere, along with a review of other HE burn models(4).

We begin our technical discussion with a review of some fundamental concepts related to combustion. This is not to suggest that shock initiation is physically the same as laminar combustion, but only that the two phenomena share similar general features, as we shall see. Following Zeldovich and Frank-Kamenetski thermal theory of pre-mixed laminar flame(5), the burning can be roughly divided into two phases: heat-up and chemical reaction. The heat-up phase involves the energy transfer from the already-burned hot region to the unburned cold region, bringing the cold region to the ignition condition. Only when the unburned region has reached high enough temperature will the chemical reaction take place at a sufficient rate and liberate energy. This concept leads to simplification of many combustion problems according to the dominance of either the transport-controlled (heat-up) or the chemical-controlled (reaction) process. To illustrate the relative importance of the two processes, we define the condition of a combustible material as a mixture of three distinct states: cold C, hot H, and burned B; each mass point contains

some or all of the states. The processes of transformation from one state to the other are:

$$C \rightarrow H \qquad \text{heat-up} \quad . \qquad (1)$$

$$H \rightarrow B \qquad \text{chemical reaction} \quad . \qquad (2)$$

Following the chemical kinetics principle(6), with t being the time, the rates of the transformations can be written as:

$$\frac{dC}{dt} = - \frac{C}{\tau_h} \quad , \qquad (3)$$

$$\frac{dH}{dt} = \frac{C}{\tau_h} - \frac{H}{\tau_r} \quad , \qquad (4)$$

$$\frac{dB}{dt} = \frac{H}{\tau_r} \quad , \qquad (5)$$

where C and H represent the mass fractions of the material in cold and hot conditions and B is the burned portion with:

$$C + H + B = 1 \quad . \qquad (6)$$

Here τ_h and τ_r are the heat-up and chemical reaction characteristic times. The rate expression of Eq. (3) is based on the assumption that the energy transfer process is a volume rather than a surface effect. The chemical reaction given in Eq. (4) represents a first-order process; with constant τ_h and τ_r, the integration of Eqs. (3) through (5) with initial conditions C=1, and H=B=0 yields

$$B = 1 + [\frac{\tau_h}{\tau_r} \exp(- \frac{t}{\tau_h}) - \exp(- \frac{t}{\tau_r})]$$

$$/(1 - \frac{\tau_h}{\tau_r}) \quad . \qquad (7)$$

If the heat-up process is much slower than the chemical process, namely, $\tau_h \gg \tau_r$, then we have the following extreme

$$B = 1 - \exp(- \frac{t}{\tau_h}) \quad . \qquad (8)$$

The other limiting case occurs when the chemical process is much slower than the heat-up process, $\tau_r \gg \tau_h$, and

$$B = 1 - \exp(-\frac{t}{\tau_r}) \quad . \tag{9}$$

Equations (8) and (9) each represents a single-rate controlled process, either thermal-mechanical or chemical. The single-step process is certainly simpler than the two-step case, and it is to our advantage to recognize when we have the former. When both characteristic times are comparable, the more general representation is the only acceptable one. In the following section, hot-spot formation, decomposition, energy transfer, etc. are considered from a general viewpoint, and then the relevant characteristic times are compared in order to reduce the entire system to a simpler, two-rate controlled process.

THE GENERAL MODEL

The heterogeneous nature of high explosives is widely recognized, as we have already discussed. The concepts of hot spots and the mechanisms leading to heterogeneous reaction are adiabatic gas compression(7), rapid shear(8), visco-plastic flow(9), void collapse(10), friction(11), and others. It is reasonable to anticipate that hot spots behave quite differently from the rest of the explosive, as far as responding to the shock action is concerned. Although adiabatic compression (pressure work) is a means of increasing the internal energy in general, dissipation associated with the irreversible stresses from the shock process is quite significant in the highly localized regions of heterogeneous material. The internal energy is increased even more and thus the temperature is much higher than the surroundings. The local high temperature starts the chemical process sooner than in the surrounding near-reversibly compressed portion. Accordingly, we divide the explosive into two major regions: the hot spots and the balance of explosive. Since we do not intend to include the details of the hot-spot formation here, we define the hot spots only in a very general way: there are sites within the HE that are potentially susceptible to mechanical stimulation (shock) and become energetic. These chemically unstable sites then proceed to decompose at a rate determined by a higher local temperature; we say that the hot spots have reached the ignition condition. Here the shock process is equivalent to the heat-up phase discussed earlier in relation to the pre-mixed flame. The balance of explosive responds to the shock in quite a different way. There are possibly some initial physical

and/or chemical changes but no substantial exothermic chemical reaction. Only after a certain amount of hot-spot reaction can additional reaction propagate into the balance of the explosive. In summary, we propose the following major steps in shock-induced chemical reaction of heterogeneous explosives:
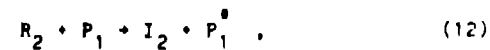
1. hot-spot creation, formation of ignition state

$$R_1 \rightarrow I_1 \quad . \tag{10}$$

2. hot-spot decomposition, consumption of ignition state

$$I_1 \rightarrow P_1 \quad . \tag{11}$$

3. heating of the balance of explosive by the hot-spot burned product, creation of the ignition state for that region

$$R_2 + P_1 \rightarrow I_2 + P_1^* \quad . \tag{12}$$

4. decomposition of the balance of explosive

$$I_2 \rightarrow P_2 \quad . \tag{13}$$

The symbols R, I, and P represent reactants, intermediates, and products; subscripts 1 and 2 are hot spots and balance of explosives, respectively. Here P_1^* represents P_1 at a cooler condition following energy transfer from the hot spots to the balance of explosive. The first two steps involve the hot spots only, but the last two control the burn in the balance of the explosive as a result of the hot-spot burn. We call this phase the burn propagation. The burn propagation plays an extremely important role, namely, the overall burning is determined by the ability of the hot spots to transfer energy to the balance of the explosive. It is further assumed that the hot-spot burn must exceed a certain threshold value to start the reaction in the balance of explosive. This leads to ignition delay in the burning of the explosive as a whole. Therefore, the critical pathway leading to the complete burning of the HE is the propagation, step 3, without which burning will be confined to the hot spots. Since the hot-spot region is usually quite small, the HE as a whole can be considered unburned if there is no propagation at all or

3

if it takes too long. The failure of burn propagation is basically the failure of transition from shock to detonation.

Let us define R_1, I_1, and P_1 to be the actual mass fractions of reactants, intermediates, and products in hot spots divided by μ, the fraction of material capable of being excited by the shock. We call these quantities normalized mass fractions and adopt similar definitions for R_2, I_2, and P_2 with $(1 - \mu)$ replacing μ in the normalizing process for the balance of explosive. Using the conventional formulation in chemical kinetics (6), we obtain the time rates of change for the processes (10) through (13):

A. the consumption rate of the unactivated hot spots due to the shock action:

$$\frac{dR_1}{dt} = -\frac{R_1}{\tau_s} \quad , \tag{14}$$

B. the creation and consumption of the ignition state of hot spots:

$$\frac{dI_1}{dt} = \frac{R_1}{\tau_s} - \frac{I_1}{\tau_c} \quad , \tag{15}$$

C. the creation of the hot-spot burned product:

$$\frac{dP_1}{dt} = \frac{I_1}{\tau_c} \quad . \tag{16}$$

D. the rate of consumption of the balance of explosive due to heating from the already burned hot spots:

$$\frac{dR_2}{dt} = -\mu \frac{R_2}{\tau_m} \left(\frac{P_1 - f_0}{1 - f_0} \right) \quad , \tag{17}$$

E. the creation and consumption of the ignition state of the balance of explosive:

$$\frac{dI_2}{dt} = \mu \frac{R_2}{\tau_m} \left(\frac{P_1 - f_0}{1 - f_0} \right) - \frac{I_2}{\tau_c} \quad , \tag{18}$$

F. the creation of the final product of the balance of explosive:

$$\frac{dP_2}{dt} = \frac{I_2}{\tau_c} \quad . \tag{19}$$

At any instant, the total unburned and burned fractions are

$$R = \mu R_1 + (1 - \mu)R_2 \quad , \tag{20}$$

$$P = \mu P_1 + (1 - \mu)P_2 \quad . \tag{21}$$

The mass fraction of hot spots μ is quite likely related to the microstructural properties such as the grain specific area and some characteristic thickness in the hot-spot region. The threshold f_0 is the normalized mass fraction of hot-spot reaction that must be reached before the burn can propagate into the balance of explosive. Equations (17) and (18) also contain the multiplication factor μ: this represents a condition that a vanishingly small mass fraction of hot spots would be incapable of inducing large scale reaction in the balance of explosive. We assume constant μ and f_0. For the normalized mass fractions,

$$R_1 + I_1 + P_1 = 1 \quad , \tag{22}$$

$$R_2 + I_2 + P_2 = 1 \quad . \tag{23}$$

In equations (14) and (15), τ_s represents the characteristic time for hot-spot excitation due to first-shock effect. If hot-spot temperature is chosen as the parameter representing the excited state, then τ_s is the characteristic time of the process leading to that temperature. It is quite likely a function of the shock strength and the material properties. The decomposition process in the ignition state is characterized by τ_c and is usually a function of the local temperature. The characteristic time τ_m controls the transport process for the energy transfer from the burned product of the hot spots to the cold balance of explosive. The mechanism of the energy transfer is possibly a turbulent mixing process at higher pressure range and simple heat conduction when the burning is less intense. It could be a function of pressure and temperature. The phenomenological correlations of these characteristic times will be described later.

4

Finally, τ_c' is the characteristic time for decomposition in the balance of explosive once the energy transfer from the hot spots has taken place.

Equation (17) deserves some additional explanation. Due to the normalized nature of the quantities R_1, R_2, I_1, I_2, P_1, and P_2, the presence of μ is required to give the absolute influence of the hot-spot mass fraction; $(1-f_0)$ is another normalizing factor so that when the hot spots have burned completely $(P_1=1)$, the threshold effect vanishes and only the energy transfer mechanism through τ_m controls the rate.

THE SPECIFIC MODEL

We now use some physical arguments to simplify the above formulation. First, in the hot-spot region, we can expect the shock (thermal-mechanical) process to be much faster than the decomposition, $(\tau_c \gg \tau_s)$, and this should lead to an instantaneous change of R_1 from one to zero. Mathematically, Eqs. (14),(15), and (16) are replaced by a single rate equation:

$$\frac{dP_1}{dt} = \frac{1}{\tau_c} \ (1 - P_1) \quad , \tag{24}$$

and from Eq. (22):

$$P_1 + I_1 = 1 \quad . \tag{25}$$

In the balance of explosive, the energy transfer (thermal-mechanical) process is expected to be much slower than the decomposition process that follows; i. e., $\tau_m \gg \tau_c'$, so we can make additional simplification that $I_2 = 0$, and from Eq. (23):

$$P_2 + R_2 = 1 \quad . \tag{26}$$

The consequence is again a single rate-controlled process:

$$\frac{dP_2}{dt} = \frac{\mu}{\tau_m} \ (1 - P_2)\left(\frac{P_1 - f_0}{1 - f_0}\right) \quad . \tag{27}$$

The overall burned product rate equation is a summation of Eqs. (24) and (27) with the use of Eq. (21):

$$\frac{dP}{dt} = \frac{\mu}{\tau_c} \ (1 - P_1)$$

$$+ \frac{\mu}{\tau_m} \ [(1 - P)-\mu(1 - P_1)]\left(\frac{P_1 - f_0}{1 - f_0}\right) \quad . \tag{28}$$

Equation (28) contains an unknown P_1 which is evaluated separately using Eq. (24). As we can see in Eqs. (24) and (28), if τ_c is much less than τ_m, (i. e., the reaction in the hot spots is much faster than the rest of the explosive, a condition that may be reached at high pressures), P_1 will reach unity much sooner than P, this will eventually lead to a single equation for the total burned mass fraction:

$$\frac{dP}{dt} = \frac{\mu}{\tau_m} \ (1 - P) \quad . \tag{29}$$

This specific case is representative of reaction-rate models such as Forest Fire[3] in which μ/τ_m is specified as a function of pressure. The specific model described in the remainder of this paper is not of this form, but rather the explicit two-step process represented by Eqs. (24) and (28).

The relationship between the two characteristic times, τ_c and τ_m, and thermal-mechanical and chemical properties of the explosive are presented in detail elsewhere[4], of which we give here only a summary.

The passage of the initial shock wave of pressure amplitude p_s produces an average hot-spot temperature θ_s given by

$$\theta_s = \theta_0\left[1 - m\frac{\theta_0}{\alpha} \ln \ \left(\frac{p_s}{p_0}\right)\right]^{-1} \quad . \tag{30}$$

where m, θ_0 and p_0 are constant and α is the Arrhenius activation temperature. For hot-spot temperature θ_s there is an induction time for thermal explosion which we identify with the characteristic time τ_c:

$$\tau_c = \frac{\theta_s^2}{\alpha \beta Z} \exp(\frac{\alpha}{\theta_s}) \quad . \qquad (31)$$

In Equation (31), β is the temperature coefficient due to chemical reaction and Z is the frequency factor for Arrhenius reaction. The quantity that is experimentally determined is the average delay for a given shock pressure. The justification for identification of τ_c in Eq. (24) with the induction time for thermal explosion is given in detail in ref. (4). Equations (30) and (31) are then used to obtain the average hot-spot temperature for assumed values of α, β and Z. The latter quantities are sometimes well-known from independent measurement, but are occasionally in doubt because of extreme thermodynamic conditions reached within the hot spots. Therefore, in this work as well as the earlier one(4), the hot-spot temperature means simply that particular temperature which gives the experimentally determined delay time for a given set of Arrhenius parameters. After the shock process, any further change of θ_s will be caused by isentropic compression or expansion(4):

$$\frac{d\theta_s}{dt} = \theta_s \Gamma \kappa \frac{dp}{dt} \quad , \qquad (32)$$

with Γ being the Gruneisen coefficient and κ the isentropic compressibility, both assumed constant. Here $\frac{dp}{dt}$ is the time rate of change of pressure. Heat loss due to thermal conduction and radiation are assumed to be negligible for the application presented here.

As the hot spots burn, energy is transferred to the balance of explosive. The second phase of the burn, burn propagation, starts as soon as sufficient energy is received by the unburned explosive. We now discuss the correlation of τ_m with the thermodynamic state.

As we have mentioned earlier, τ_m represents the process of energy transfer. When the pressure is low, we expect the mechanism to be simple heat conduction, but at much higher pressure levels, convection and local mixing could be a major factor for the rapid increase of the effectiveness of energy transfer. The parameter τ_m in fact plays the role of both film coefficient and temperature difference between the hot and cold regions. Accordingly, we propose the following expression:

$$\tau_m = [G_0 p + G(p)]^{-1} \quad . \qquad (33)$$

The linear term in p represents the weaker energy transfer mechanism, most likely thermal conduction, and G is a highly nonlinear function of the current pressure p; we speculate the effect is due to the more efficient energy transfer mechanism such as turbulence. For high pressures, G provides the dominant contribution; in fact, we can identify that term to the pressure dependence in the Forest-Fire rate(3), when we compare the Forest-Fire model with Eq. (29). The determination of G is therefore carried out through a procedure similar to the Forest Fire model using Pop plot information; G_0 is obtained from the embedded gauge data and the Pop plot in the low pressure range. Using the original Forest-Fire rate function form(3),

$$G(p) = \exp(\sum_{i=0}^{n} a_i p^i) \quad . \qquad (34)$$

Since the current formulation has an explicit multiplier μ in the propagation term of Eq. (28), values of G_0 and a_0 differ from the original formulations(3,4).

The explicit hot-spot model of shock initiation represented by Eqs. (24), (28) and (30) through (32) also includes the physical effect of shock desensitization(12): A shock wave of insufficient amplitude to cause prompt initiation itself has the effect of desensitizing the explosive to additional compression. That this effect is indeed included in the model given here can be seen by starting with Eq. (30). Consider a first shock of pressure p_s that creates an average hot-spot temperature θ_s. If θ_s is small enough, the characteristic time τ_c due to the first shock is too long. Additional heating due to subsequent shocks takes place according to the adiabatic relationship, Eq. (32), which is much less efficient than Eq. (30) for producing high hot-spot temperatures. The physical explanation for this is that hot-spot creation is a highly irreversible and dissipative process, and can happen only once when the first shock arrives. Subsequent shocks can do only reversible mechanical work on relatively cool hot spots that have already been formed.

Figure 1 gives a quantitative description of this phenomenon for PBX-9404 (94% HMX/3% NC/3% CEF) with various values of Γκ in Eq. (32). The discussions are general and apply to explosives other than PBX-9404. Figure 1 gives the average induction time for hot-spot

6

reaction for a 5-GPa second shock preceeded by a first shock of amplitude p_s. For a single 5-GPa shock, the induction time is ~0.2 µs; point A on the solid line given by Eqs. (30)and (31) with p_s=5 GPa. If the 5-GPa shock is preceeded by a 1-GPa shock, the induction time for the first shock (1 GPa) is ~11 µs, point B. If $\Gamma\kappa$=0, there is no additional heating due to the second shock and the induction timeremains at ~11 µs. If $\Gamma\kappa$ = 0.01 GPa^{-1}, the induction time is reduced to 4 us, point C; this is still quite long compared to ~0.2 µs for a single 5-GPa shock. As the compressibility is increased, the delay time behind the second shock gets closer to that for a single shock (points D and E in comparison with A). The dashed lines in Fig. 1 are the delay times behind a 5-GPa shock that follows a first shock of amplitude p_s.

These delay times increase significantly as p_s is decreased until a threshold shock pressure is reached (below which hot spots cannot be created by the first shock). Below this threshold (not shown) the second shock travels into essentially virgin material and the delay time decreases rapidly to a value near that for a single shock (i. e., point A for a single 5-GPa shock).
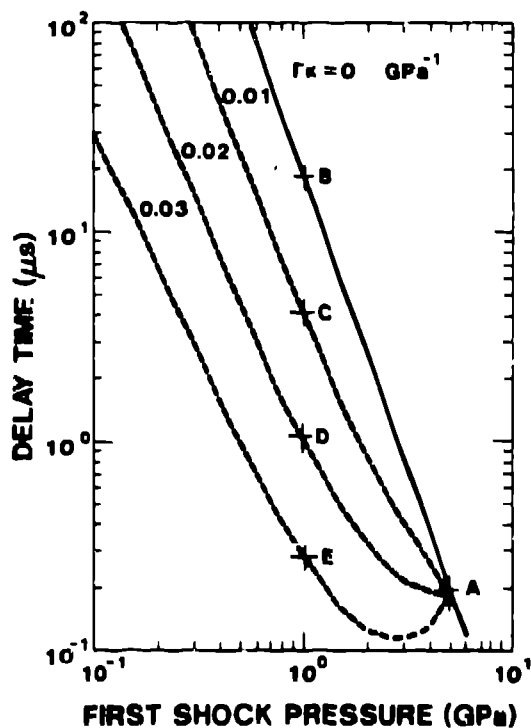
COMPUTATIONAL RESULTS

Calibration of the explicit hot-spot model presented here is described in detail in (4) for sustained impact in PBX-9404. Computations were performed numerically by the method of characteristics tracking a single discontinuous shock front. A thick lucalox impactor produced an initial particle velocity of 0.055 cm/µs in the PBX-9404 sample, experiment 547(13). Comparison of the theoretical calculation with measured particle velocities at 0.5 mm, 2.5 mm, and 4.5 mm is shown in Fig. 2. The same model was used with identical rate parameters to compare with measured particle velocitie. for a finite-duration pulse. In experiment 532(13), a 0.28-cm thick lucalox projectile produces a 0.51-us pulse with initial particle velocity of 0.053 cm/µs in PBX-9404. Comparison of theory and experiment is shown in Fig. 3 for particle velocity gauges located at 0.2 mm, 1.2 mm, and 3.2 mm. The good agreement shown in Fig. 3 is very encouraging because calibration was performed for a sustained shock, Fig. 1. This result gives some

Figure 1. Effect of the first shock on the delay time followed by a second 5-GPa shock.
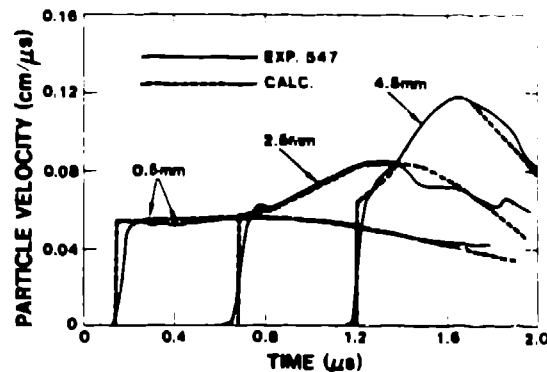

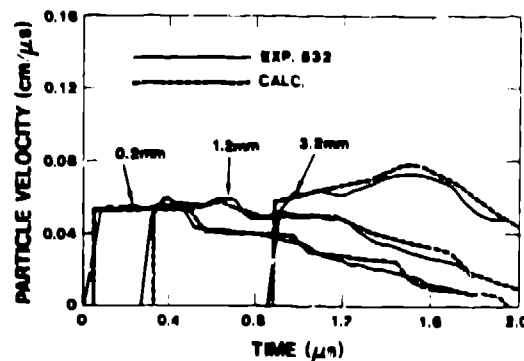Figure 2. Sustained impact results, experiment and calculation.

Figure 3. Finite-duration pulse results, experiment and calculation.

confidence that the explicit hot-spot model represents reasonable departures from calibration situations. As obvious a requirement as this may be for shock initiation models, it has not always been demonstrated.

We have also included the explicit hot-spot model in the two-dimensional, hydrodynamic finite-element code DYNA2D(14). As one check of the explicit hot-spot model and the code, a number of distance-to-detonation calculations were performed and compared with the characteristic theory and the experimental data, the results are shown in Fig. 4. In addition to these comparisons, DYNA2D showed favorable comparison with the data and characteristic calculation given in Fig. 2.
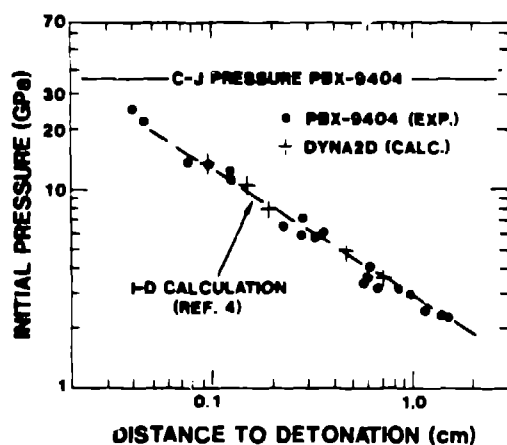

Figure 4. Pop plot for PBX-9404, experiment, 1-D and 2-D calculations.

In the remainder of the work described here, the DYNA2D code with the explicit hot-spot burn model was used to investigate two-dimensional effects of corner turning and shock desensitization in PBX-9502 (95% TATB /5% Kel-F). The model parameters for PBX-9502 were estimated from the Pop plot given in (15) and embedded gauge measurements for porous TATB(16), which give an approximate value of τ_c ~1 μs for a shock pressure of ~8 GPa. The Arrhenius constants for TATB are given in (17).

For the case of corner turning when the explosive changes size abruptly, we use a 2-cm long PBX-9404 booster to start the burn in PBX-9502. The explicit hot-spot burn model is used for PBX-9502 but programmed burn is imposed on PBX-9404. The problem configuration is given in Fig. 5 with the explosives bound by plexiglas. With a radius of 1.3 cm in the first segment (4-cm long) and 6-cm radius in the second segment (3-cm long), the burned mass fraction contours are shown in

Fig. 6 at 14 μs, a partially burned region is seen near the region where the explosive increases suddenly in size. The reason for this behavior is the rapid lowering of shockpressure when the detonation wave tries to expand suddenly, resulting in partial burn or even complete extinction, at least in some local region. However, the main burn front is still strong enough to maintain the burn so that an expanding detonation wave can be formed eventually, except the portion in the vicinity of the corner.
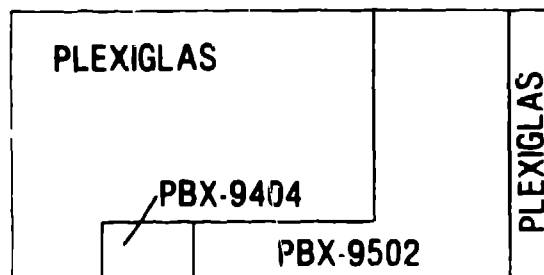

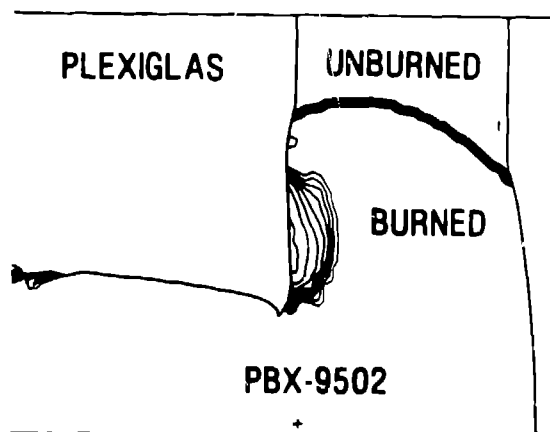Figure 5. Configuration for corner turning simulation.

Figure 6. Burned mass fraction contours for a detonation wave turning a corner in PBX-9502.

The final example is a study of shock desensitization, using the configuration of Fig. 5 but replacing the material bounded on the side with aluminum. A weak shock will travel through that medium and reach part of the explosive block sooner than the main detonation front because of the higher shock velocity for aluminum. Since the intensity of the shock is weak, the initial hot-spot temperature associated with the shock remains low and the ignition delay is very long. Even with subsequent compression of high intensity, the ignition delay is not reduced enough to cause significant burn in the hot-spot region

as discussed earlier. The effect of the pre-
shock on the burned mass fraction (P) at 14
µs is shown in Fig. 7; a well-defined unreacted
region is seen between the aluminum and
PBX-9502. Figure 8 shows the density contours
exhibiting the sharp contrast of the density
between the burned and unburned regions. A
flash radiograph of shot no. 1746(18) for PBX-
9502 turning a 90-deg aluminum corner is
reproduced in Fig. 9. Although the experiment
was performed with a somewhat different
geometry, the essential features are
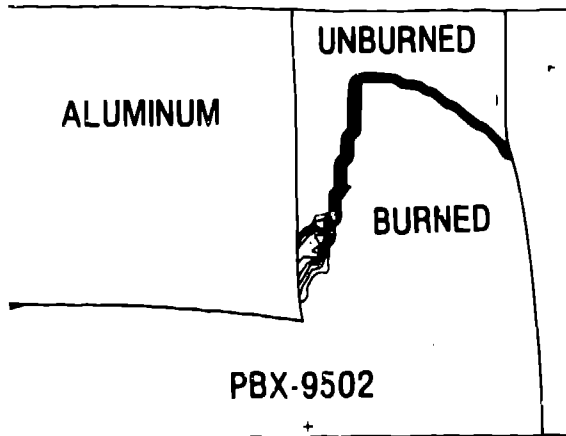reproduced by the explicit hot-spot model.

Figure 7.   Burned mass fraction contours
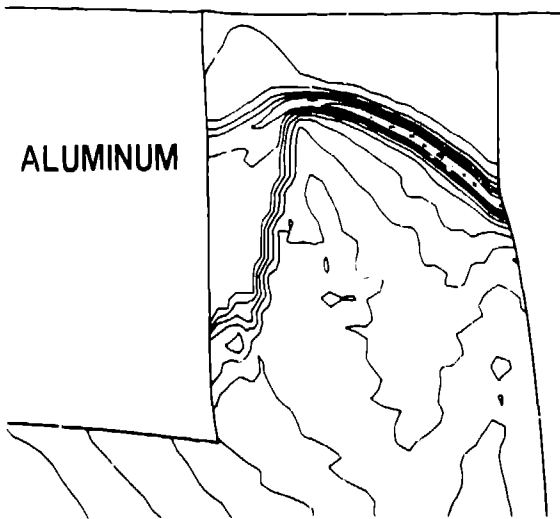for PBX-9502 with shock
desensitization.

Figure 8.   Density contours showing the
effect of shock
desensitization.

Figure 9.   Flash radiography.

CONCLUSION

We have presented a new HE burn model and
demonstrated some of the experimentally
observed features of the model in one and two
dimensions. The resul. · are quite encouraging
and we shall continue the effort; in
particular, we shall investigate further how
those empirical parameters relate to the
thermodynamic state and material properties
such as initial temperature and grain size.
The energy transfer concept of this model
prompts us to believe that those parameters
θ_0, f_0, G_0, and a_i's must be related to the
initial temperature. The hot-spot mass
fraction, u, must be linked to the grain size
through the surface area and inter-granular
inhomogeneity; a smaller grain size would
result in a larger hot-spot mass fraction.
Therefore it is possible that finer grain size
may lead to shorter run distances as some
experiments indicate(12). However, the grain
size may also have some effect on the initial
reference hot-spot temperature. As the grains
become smaller, the material approaches a more
homogeneous state which reduces the
dissipation coming from the irreversible
stress components. The net effect is a lower
reference hot-spot temperature θ_0 which would

decrease the hot-spot burn rate, resulting in
longer run distance. Experimental evidence
also supports this trend at low shock
pressures(19). At the present time, the data
needed for the model are limited and in some
cases, preliminary. More experimental work is
required to support the model improvement and
actual application.

REFERENCES

1. W. Fickett and W. Davis, Detonation, pp. 16-20, University of California Press, Berkeley, 1979.

2. J. B. Ramsay and A. Popolato, "Analysis of Shock Wave and Initiation Data for Solid Explosives," pp. 233-288, Fourth Symposium on Detonation, ACR-126, 1965.

3. C. Mader and C. Forest, "Two-Dimensional Homogeneous and Heterogeneous Detonation Wave Phenomena," Los Alamos Scientific Laboratory Report, LA-6259, June 1976.

4. J. Johnson, P. Tang, and C. Forest, "Shock-Wave Initiation of Heterogeneous Reactive Solids," Journal of Applied Physics, to appear.

5. A. Kanury, Introduction to Combustion Phenomena, pp. 297-300, Gordon and Beach, New York, 1975.

6. F. Williams, Combustion Theory, pp. 361, Addison-Wesley, Reading, 1965.

7. J. Starkenberg, "Ignition of Solid High Explosive by the Rapid Compression of an Adjacent Gas Layer," Seventh Symposium (International) on Detonation, NSWC MP 82-334, pp. 3-16, June 1981.

8. R. Frey, "The Initiation of Explosive Charges by Rapid Shear," Seventh Symposium (International) on Detonation, NSWC MP 82-334, pp. 36-42, June 1981.

9. B. Khasainov, A. Borisov, B. Ermolaev, and A. Korotkov, "Two-Phase Visco-Elastic Model of Shock Initiation in High Density Pressed Explosives," Seventh Symposium (International) on Detonation, NSWC MP 82-334, pp. 435-447, June 1981.

10. Y. Partom, "A Void Collapse Model for Shock Initiation," Seventh Symposium (International) on Detonation, NSWC MP 82-334, pp. 506-516, June 1981.

11. J. Dienes, "Frictional Hot-Spots and statistical Crack Mechanics," 1983 Annual Meeting of Material Research Society, Nov. 1983.

12. A. Campbell, W. Davis, J. Ramsay, and J. Travis, "Shock Initiation of Solid Explosives," Physics of Fluids, Vol. 4, No. 4, pp. 511-521, April 1961.

13. J. Vorthman, personal communication.

14. J. Hallquist, "User's Manual for DYNA2D -- An Explicit Two-Dimensional Hydrodynamic Finite Element Code with Interactive Rezoning," Lawrence Livermore National Laboratory, UCID-18756, Feb. 1982.

15. T. Gibbs and A. Popolato, LASL Explosive Data, pp. 397-399, University of California Press, Berkeley, 1980.

16. A. Anderson, M. Ginsberg, W. Seitz, and J. Wackerle, "Shock Initiation of TATB," Seventh Symposium (International) on Detonation, NSWC MP 82-334, pp. 385-393, June 1981.

17. R. Rogers, "Thermochemistry of Explosives", Thermochimica Acta, Vol. 11, pp. 131-139, 1975.

18. C. Mader, ed., LASL PHERMEX Data, Volume III, pp. 463, University of California Press, Berkeley, 1980.

19. R. Setchell, "Grain-Size Effects on the Shock Sensitivity of Hexanitrostilbene (HNS)," Combustion and Flame, Vol. 56, No. 3, pp. 343-345, June 1984.